

PAPER • OPEN ACCESS

Exsolution Enhancement of Metal-support CO Oxidation Perovskite Catalyst with Parameter Modification

To cite this article: G L Lew *et al* 2021 *IOP Conf. Ser.: Earth Environ. Sci.* **765** 012078

View the [article online](#) for updates and enhancements.

You may also like

- [PEO-LiN \(SO₂CF₂CF₃\)₂ Polymer Electrolytes: I. XRD, DSC, and Ionic Conductivity Characterization](#)
G. B. Appetecchi, W. Henderson, P. Villano et al.
- [Evidence that 50% of BALQSO Outflows Are Situated at Least 100 pc from the Central Source](#)
Nahum Arav, Guilin Liu, Xinfeng Xu et al.
- [Probing the Outflowing Multiphase Gas 1 kpc below the Galactic Center](#)
Blair D. Savage, Tae-Sun Kim, Andrew J. Fox et al.

PRIMETM
PACIFIC RIM MEETING
ON ELECTROCHEMICAL
AND SOLID STATE SCIENCE

HONOLULU, HI
October 6-11, 2024

Joint International Meeting of
The Electrochemical Society of Japan (ECSJ)
The Korean Electrochemical Society (KECS)
The Electrochemical Society (ECS)

Early Registration Deadline:
September 3, 2024

**MAKE YOUR PLANS
NOW!**

Exsolution Enhancement of Metal-support CO Oxidation Perovskite Catalyst with Parameter Modification

G L Lew¹, N Ibrahim², S Abdullah³, W R Wan Daud^{4,5} and W K W Ramli^{1*}

¹Faculty of Chemical Engineering Technology, Universiti Malaysia Perlis (UniMAP), Perlis, Malaysia.

² Faculty of Civil Engineering Technology, Universiti Malaysia Perlis (UniMAP), Perlis, Malaysia.

³ Faculty of Chemical and Natural Resources Engineering, Universiti Malaysia Pahang (UMP), Pahang, Malaysia.

⁴ Department of Chemical Engineering and Process, Research Centre for Sustainable Process Technology, Universiti Kebangsaan Malaysia (UKM), Selangor, Malaysia.

⁵ Fuel Cell Institute, Universiti Kebangsaan Malaysia (UKM), Selangor, Malaysia.

E-mail: wankhairunnisa@unimap.edu.my

Abstract. This study aimed to further tune the capability of active metal exsolution onto the surface of the CO oxidative perovskite catalyst $\text{La}_{0.7}\text{Ce}_{0.1}\text{Co}_{0.3}\text{Ni}_{0.1}\text{Ti}_{0.6}\text{O}_3$ by tuning the reducing parameter. Under same calcination temperature of 800°C, XRD analysis shown that the precursors with calcination duration of 6 hours ($\text{S}_2\text{T}_8\text{H}_6$) was able to achieve similar crystalline structure to those with calcination duration of 12 hours ($\text{S}_2\text{T}_8\text{H}_{12}$). In order for the active metal (CoNi) to be exsolved onto the perovskite surface, reducing parameter such as temperature and duration are deemed crucial to the reduction process. The exsolution of the active metals was observed when the samples were treated under reducing condition with varying temperatures of 550°C and 700°C and duration from 200 to 300 minutes. Through comparison with their EDX readings, $\text{S}_2\text{T}_8\text{H}_6$ treated under 700°C and 300 minutes ($\text{S}_2\text{T}_8\text{H}_6\text{-R}_7\text{H}_5$) achieved the highest weight percentage of surface Cobalt and Nickel of 3.83 and 2.81. It was clear that by tuning the temperature and duration of reduction, the exsolution of the active metals onto the surface of the perovskite could be improved resulting in better exposure and dispersion of active metals onto the surface of catalyst.

1. Introduction

Carbon monoxide (CO), being one of the many hazardous flue gases that is capable of causing respiratory system malfunction and this CO is predominately produced through incomplete combustion of carbon-containing compounds such as vehicle fuels or agricultural waste [1]. Heterogeneous oxidative catalysts had been used to overcome the discharge of CO by converting CO into a much less hazardous gases, carbon dioxide (CO_2) [2]-[3]. Oxidative catalysts commonly consist of metal or alloy deposited, impregnated or precipitated onto a supporting material and activated via oxidation or reduction prior to the catalytic reaction. Ideally, catalysts used should exhibit long-term stability and efficiency throughout the process but in reality, catalysts often suffer from catalyst poisoning, inhibition of active sites, particle agglomeration or sintering reducing the lifetime of catalysts [4].

Perovskite oxide are consist of a nominal composition of ABO_3 where it can accommodate two metal ions A and B where A usually a larger ionic radius alkali earth metals and B, being a smaller ionic radius



Content from this work may be used under the terms of the [Creative Commons Attribution 3.0 licence](https://creativecommons.org/licenses/by/3.0/). Any further distribution of this work must maintain attribution to the author(s) and the title of the work, journal citation and DOI.

metal ion that can be substituted with high catalytical elements to become a perovskite catalyst suitable for various application [5]. In order for perovskite structure to remain stable, the radius of the perovskite ions have to fall under the tolerance factor t ($0.75 < t < 1$) [6]. The ideal perovskite structure is in cubical form but with the broad constraints of time, t , perovskite oxide exhibit good elemental adjustability with a cost of slight distortion of lattice structure [7].

With the unique structure of perovskite oxide, the substituted high catalytical element could be elevated from the lattice structure onto the surface of perovskite structure through exsolution by exposing the perovskite structure in a reducing environment forming a fine dispersion of firmly anchored nanoparticles on the surface of catalyst [8]. Unlike the conventional deposition methods, exsolution could be done in a more cost-effective way and does not require plenty expensive precursors to produce a fine and well dispersed nanoparticle [9]. Furthermore, the exsolved nanoparticles proved to have better sintering stability and even after active nanoparticles were oxidized, the perovskite catalyst could extend its lifetime by undergoing another reduction process in order to regrow the active nanoparticles, showing the long lifetime and reusability of the perovskite catalyst [10].

Hence, this study sought to identify the structure of a $\text{La}_{0.7}\text{Ce}_{0.1}\text{Co}_{0.3}\text{Ni}_{0.1}\text{Ti}_{0.6}\text{O}_3$, a CO oxidative perovskite catalyst, with cobalt nickel (CoNi) as the reactive metal. Furthermore, the effects of reducing parameters such as reducing temperature and duration on the exsolution of CoNi was also studied. The fabricated $\text{La}_{0.7}\text{Ce}_{0.1}\text{Co}_{0.3}\text{Ni}_{0.1}\text{Ti}_{0.6}\text{O}_3$ nanoparticles were characterized using X-ray diffraction (XRD) to identify the formation of pure perovskite structure and its structural properties, while the exsolution of CoNi was observed through Scanning Electron Microscope (SEM). Energy Dispersive X-ray (EDX) was used to identify the presence of exsolved CoNi and quantify the distribution of CoNi exsolution through the modification of the reducing parameters.

2. Materials and methods

2.1. Chemical and gases

99.98% Lanthanum oxide (La_2O_3), 99.9% Ceria oxide (CeO_2), Titanium oxide (TiO_2) and 99% Nickel (II) nitrate hexahydrate ($\text{Ni}(\text{NO}_3)_2 \cdot 6\text{H}_2\text{O}$) were purchased from Acros Organics, United States while 99.5% Cobalt (III) oxide (Co_3O_4) was purchased from Sigma-Aldrich, United States. The gases used include 30% hydrogen/argon (H_2/Ar) and 99.999% nitrogen (N_2) were purchased from Linde group, Ireland. All chemicals and gases for experimental works were used without additional purification.

2.2. Sample Preparation

The CO oxidative perovskite catalysts, $\text{La}_{0.7}\text{Ce}_{0.1}\text{Co}_{0.3}\text{Ni}_{0.1}\text{Ti}_{0.6}\text{O}_3$ were fabricated through a modified solid-state reaction method proposed by Wan Ramli et al. [10]. The precursors including La_2O_3 , CeO_2 , Co_3O_4 , $\text{Ni}(\text{NO}_3)_2 \cdot 6\text{H}_2\text{O}$ and TiO_2 were first weighed and well mixed. The mixture was then calcined in a primary calcination process at 1000°C for 12 hours. The powders were then collected and fired again under 800°C but at two different duration of 6 hours and 12 hours, producing $\text{S}_2\text{T}_8\text{H}_6$ and $\text{S}_2\text{T}_8\text{H}_{12}$. The samples were then reduced under H_2 in a conventional continuous flow reactor for the exsolution tuning process to happen. The conventional continuous flow reactor used consisted of a quartz fixed-packed bed reactor with gases supply connected with mass flow controller (MFC) as depicted in Figure 1.

The samples were placed in between two supporting quartz wool to ensure the sample remained at the center of the heating element before connecting it with the gases supply. The gases were supplied into the reactor through a bottom-top direction. The metals exsolution was done under varying reducing conditions with a continuous 20 ml/min flow of 30% H_2/Ar at 700°C and 500°C , as listed in Table 1, in order to compare the effects of reducing conditions toward the exsolution of CoNi. Before each reduction, the quartz reactor was flushed with 150 ml/min of N_2 with the temperature of 150°C to remove excess moisture in the reactor prior to the reduction.

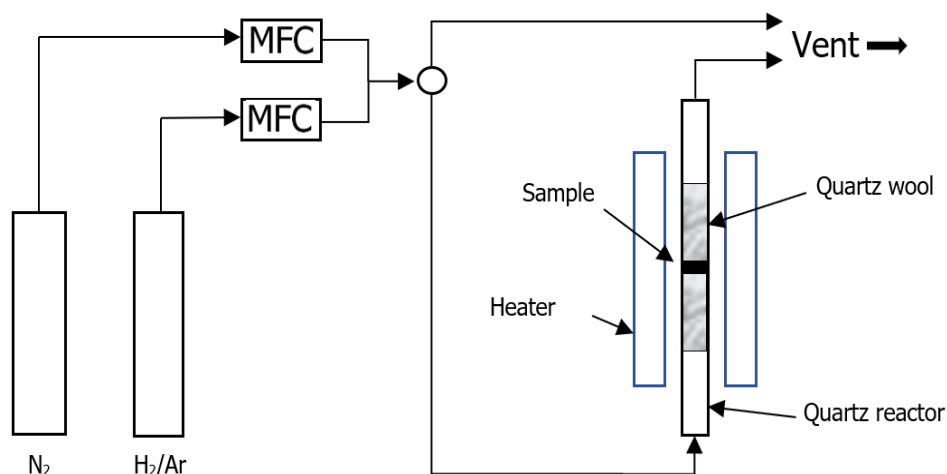


Figure 1. Experimental set up for the exsolution process.

Table 1. $\text{La}_{0.7}\text{Ce}_{0.1}\text{Co}_{0.3}\text{Ni}_{0.1}\text{Ti}_{0.6}\text{O}_3$ samples with their treatment stages and conditions.

Sample	Stage	Conditions
$\text{S}_2\text{T}_8\text{H}_6$	Secondary Calcination	$T = 800^\circ\text{C}$, calcined for 360 minutes
$\text{S}_2\text{T}_8\text{H}_{12}$		$T = 800^\circ\text{C}$, calcined for 720 minutes
$\text{S}_2\text{T}_8\text{H}_6\text{-R}_7\text{H}_3$	Reduction Process	$T = 700^\circ\text{C}$, reduced for 200 minutes
$\text{S}_2\text{T}_8\text{H}_6\text{-R}_7\text{H}_4$		$T = 700^\circ\text{C}$, reduced for 250 minutes
$\text{S}_2\text{T}_8\text{H}_6\text{-R}_7\text{H}_5$		$T = 700^\circ\text{C}$, reduced for 300 minutes
$\text{S}_2\text{T}_8\text{H}_6\text{-R}_5\text{H}_5$		$T = 500^\circ\text{C}$, reduced for 300 minutes

2.3. Sample Characterisation

The crystalline structure of the fabricated samples was analyzed using Bruker D2 Phaser benchtop X-ray diffractometer (XRD), equipped with LYNEYE 1D Ultra-fast-solid-state detector with $\text{CuK}\alpha$ radiation ($\lambda = 1.54184 \text{ \AA}$) to ensure the formation of the desired perovskite structures. The exsolution of CoNi metals onto the surface of the catalysts and the elemental distribution were evaluated using a Variable Pressure Scanning Electron Microscope (Carl Zeiss Evo Ma 10 (UK)), equipped with Energy Dispersive X-ray (EDX), Edax Apollo X (USA). Magnification

3. Results and discussion

3.1. Formation of perovskite structure

Through XRD characterization, similar peaks indicating perovskite phase was observed in both $\text{S}_2\text{T}_8\text{H}_6$ and $\text{S}_2\text{T}_8\text{H}_{12}$ [4]. The major peaks related to the pure perovskite phase were labelled with P, as shown in Figure 2. Regardless of the calcination duration, their patterns were almost indistinguishable, showing the weak effect of the duration time in this calcination process, showing that $\text{S}_2\text{T}_8\text{H}_6$ was capable to exhibit similar structures of $\text{S}_2\text{T}_8\text{H}_{12}$. A search-match was done within Crystallography Open Database (COD) to propose a similar crystal structure to $\text{S}_2\text{T}_8\text{H}_6$. The results shows that, $\text{S}_2\text{T}_8\text{H}_6$ has similar structure with most of the major peaks aligned but in slight difference in intensity to lanthanum cobalt oxide, LaCaO_3 [11]. This showed that $\text{S}_2\text{T}_8\text{H}_6$ fabricated compose of the similar structure as the LaCaO_3 which consist of a rhombohedral structure with a space group of R-c3 and lattice constant values of $a = b = 5.444 \text{ \AA}$ and $c = 13.104 \text{ \AA}$ [12]. Hence the following exsolution enhancement will be performed using $\text{S}_2\text{T}_8\text{H}_6$.

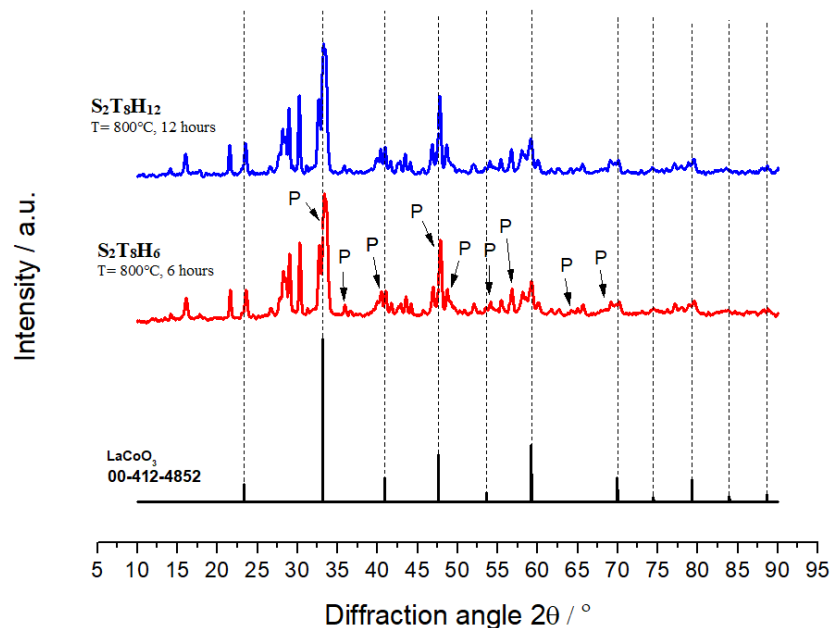


Figure 2. XRD patterns for $S_2T_8H_6$ and $S_2T_8H_{12}$ and $LaCoO_3$ COD card. P denotes the peaks indicating the presence of the perovskite phase.

3.2. The exsolution of active metal

Under reducing condition, the active metals within the perovskite structure will be elevated from the lattice structure to the surface. Figure 3 compares the exsolution of active metal (CoNi) in reduced $S_2T_8H_6$ with the untreated $S_2T_8H_6$ under SEM analysis. The exsolved CoNi on the reduced $S_2T_8H_6$ at temperature of 700°C ($S_2T_8H_6\text{-}R_7H_3$) are more visible compared to the untreated surface as CoNi are exsolved as small granular particles onto the surface of $S_2T_8H_6\text{-}R_7H_3$. The exsolution of CoNi on $S_2T_8H_6\text{-}R_7H_3$ was further supported with EDX result, where the surface of untreated have no sign of CoNi while the surface of $S_2T_8H_6\text{-}R_7H_3$ have around 1.86 wt% of Co and 0.31 wt% of Ni, present respectively. Results from the sample before exposing to the reducing environment aligned with the findings concluded by Rosen [13], as the surface of perovskite was smooth with no emerging small nanoparticle granule on the surface of perovskite but as the sample exposed to a reducing atmosphere, CoNi particles were exsolved but not as evenly distributed as mentioned in Wan Ramli et al. [10]. It was to believe that the selective exsolution of CoNi was caused by insufficient reducing temperature, causing a certain degree of restrained mobility for Co and Ni particles to form a uniformly distributed surface [2].

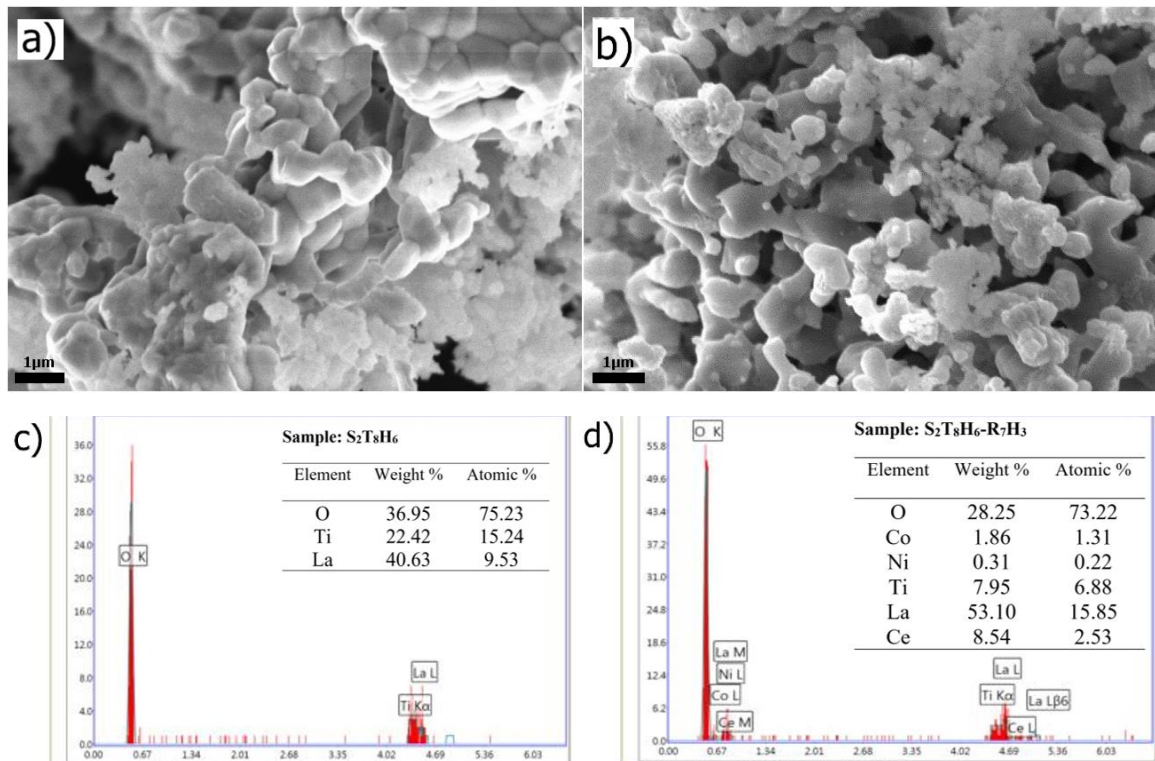


Figure 3. SEM/EDX result comparison of S₂T₈H₆ and S₂T₈H₆-R₇H₃. 10k magnification VPSEM image of (a) untreated S₂T₈H₆ and (b) treated S₂T₈H₆-R₇H₃. EDX result shows the readings of elements present on the surface of (c) S₂T₈H₆ and (d) S₂T₈H₆-R₇H₃

3.3. Effects of reducing temperature and duration on exsolution

After the exsolution, the effects of reducing duration was tested to observe the difference in CoNi exsolution onto the surface of S₂T₈H₆. Figure 4 displayed the SEM/EDX analysis of the samples S₂T₈H₆-R₅H₅ and S₂T₈H₆-R₇H₃₋₅. SEM images indicate the presence of exsolved CoNi onto the S₂T₈H₆ surface (small granule particles), supported by the EDX results shown in Table 2 indicated an increasing trend of Co and Ni weight percentages on S₂T₈H₆-R₇H₃ and S₂T₈H₆-R₇H₅. Through the research done by Naegu [14], the reducing temperature affects the particles size that exsolved onto the surface of the perovskite such as at 550°C, the reported particles size were around 10 nm and 30 nm particles size for 860°C. This explained the exsolved CoNi in R₇H₃ to R₇H₅ are more noticeable than of R₅H₅ due to the larger exsolved particle size than those exsolved onto R₅H₅ while the higher weight readings of Co and Ni on R₅H₅ may because of the smaller particle size under the same area coverage by EDX analysis have higher exposure compared to the CoNi particles in R₇H₃ and R₇H₄ that were partially elevated from their lattice.

Further characterizations are required especially in terms of evaluating the particles size and distribution since this will help in quantifying their effects in future performance testing using CO oxidation.

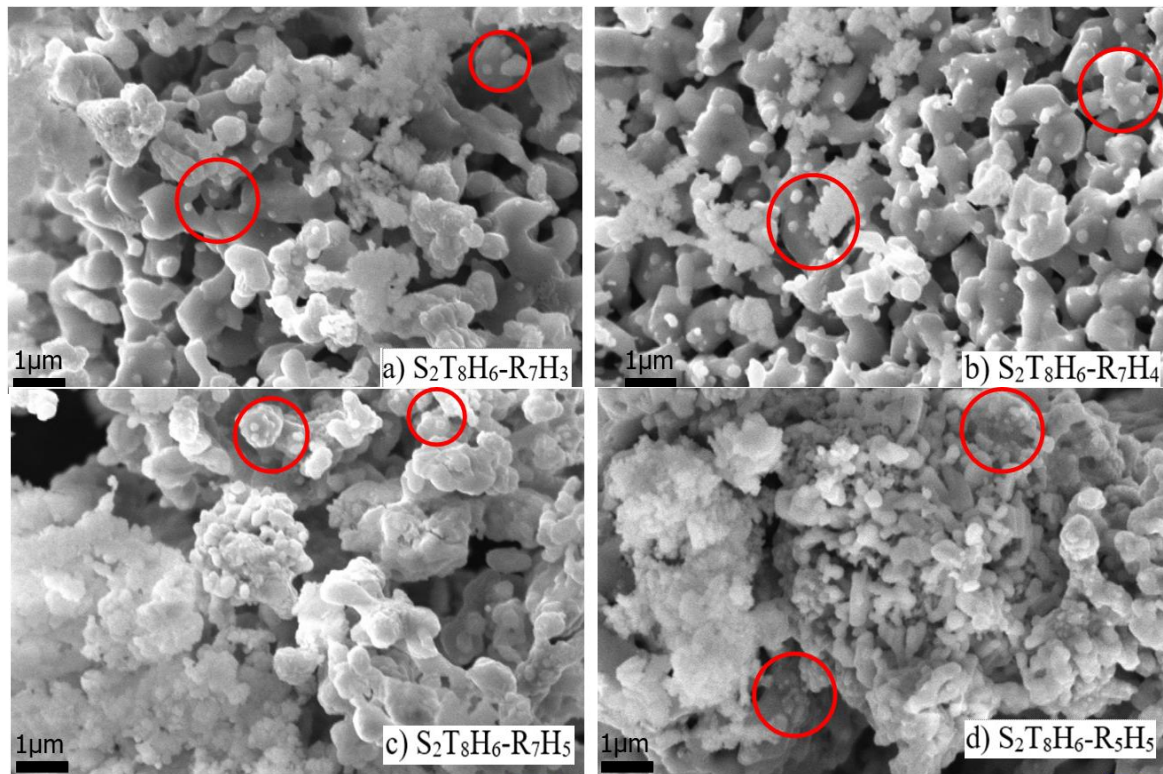


Figure 4. SEM result comparison of $S_2T_8H_6$ surface with treatment $R_{7H_{3-5}}$ and R_5H_5 . 10k magnification SEM result of $S_2T_8H_6$ with treatment of (a) R_7H_3 , (b) R_7H_4 , (c) R_7H_5 and (d) R_5H_5 .

Table 2. EDX results on Co and Ni weight and atomic percentage of fabricated samples

Sample	Element	Weight %	Atomic %
$S_2T_8H_6-R_7H_3$	CO	1.86	1.31
	Ni	0.31	0.22
$S_2T_8H_6-R_7H_4$	CO	2.22	1.74
	Ni	1.85	1.45
$S_2T_8H_6-R_7H_5$	CO	3.83	2.58
	Ni	2.81	1.90
$S_2T_8H_6-R_5H_5$	CO	3.10	1.79
	Ni	1.47	0.85

4. Conclusion

Through this study, the sample calcination temperature of 800°C ($S_2T_8H_6$) was able to obtain the pure perovskite structure required for exsolution as those calcined at temperature of 1000°C ($S_2T_{10}H_6$) showing that the effect of calcination temperature during perovskite formation is not significant. The exsolution of active metals (CoNi) was achieved with a continuous reducing condition of 700°C for 200 minutes ($S_2T_8H_6-R_7H_3$) and the exsolved CoNi particles from the perovskite lattice formed small, dispersed granular particles on to the smooth surface of $\text{La}_{0.7}\text{Ce}_{0.1}\text{Co}_{0.3}\text{Ni}_{0.1}\text{Ti}_{0.6}\text{O}_3$ was observed.

Through reducing temperature and duration modification, exsolved particles size could be controlled with reducing temperature while the exsolution of CoNi can further be tuned to have higher weight and atomic percentage as more time allocated for the reduction process to complete the exsolution. Under same reducing temperature of 700°C, S₂T₈H₆-R₇H₅ with 300 minutes reduction, the exsolution of 3.83 wt% and 2.81 wt% of Co and Ni, respectively was observed compared to R₇H₃ with 200 minutes reduction, exsolution of 1.86 wt% of Co and 0.31 wt% of Ni.

References

- [1] Duro J A 2016 *Ecol. Indic.* **66** 173–9
- [2] Park S, Kim Y, Noh Y, Kim T, Han H, Yoon W, Choi J, Yi S H, Lee W J, and Kim W B 2019, *J. Mater. Chem. A* **8(1)** 138–48
- [3] Gustafson J, Balmes O, Zhang C, Shipilin M, Schaefer A, Hagman B, Merte L R, Martin N M, Carlsson P A, Jankowski M, Crumlin E J, and Lundgren E 2018 **8** 4438–45
- [4] Lindenthal L, Rameshan R, Summerer H, Ruh T, Popovic J, Nenning A, Löffler S, Opitz A K, Blaha P, and Rameshan C 2020 **10** 1–14
- [5] Atta N F, Galal A and El-Ads E H 2016 *Perovskite Materials–Synthesis, Characterisation, Properties, and Application* 107-51
- [6] Pan K L, Chen M C, Yu S J, Yan S Y and Chang M B 2016 *J. Air Waste Manag. Assoc.* **66(6)** 619–30
- [7] Hou X, Ren J, Li F, Ma C, Zhang X and Feng H 2019 *IOP Conference Series: Earth and Environmental Science* **295(3)** 032020
- [8] Kwon O, Joo S, Choi S, Sengodan S and Kim G 2020 *J. Phys. Energy* **2(3)** 032001
- [9] Papargyriou D and Irvine J T S 2016 *Solid State Ionics* **288** 120–3
- [10] Wan Ramli W K, Papaioannou E, Naegu D and Metcalfe I S 2020 *IOP Conf. Ser. Mater. Sci. Eng.*, **778(1)** 012059
- [11] Wold A and Ward R 1954 *J. Am. Chem. Soc.* **76(4)** 1029–30
- [12] Dragan M, Enache S, Varlam M and Petrov K 2019 *Cobalt Compounds and Applications*
- [13] Rosen B A 2020 *Electrochem.* **1(1)** 32–43
- [14] Neagu D, Papaioannou E, Wan Ramli K W, Miller D N, Muroch B J, Ménard H, Umar A, Barlow A J, Cumpson P J, Irvine J T S, and Metcalfe I S 2017 *Nat. Commun.* **8(1)** 1–8

Acknowledgement

The authors would like to acknowledge the support from the Fundamental Research Grant Scheme (FRGS) under a grant number of FRGS/1/2018/TK02/UNIMAP/02/8 from the Ministry of Higher Education Malaysia (MOHE). The authors would also like to thank Centre of Excellence for Frontier Materials Research (CFMR), Universiti Malaysia Perlis (UniMAP) and Fuel Cell Institute (SELFUEL), Universiti Kebangsaan Malaysia (UKM) for assisting in samples characterizations throughout this work.